

See discussions, stats, and author profiles for this publication at: <https://www.researchgate.net/publication/236975985>

Water Dispersal and Functionalization of Hydrophobic Iron Oxide Nanoparticles with Lipid-Modified Poly(amidoamine) Dendrimers

ARTICLE in LANGMUIR · MAY 2013

Impact Factor: 4.46 · DOI: 10.1021/la400791a · Source: PubMed

CITATIONS

9

READS

86

5 AUTHORS, INCLUDING:



Adriano Boni

Istituto Italiano di Tecnologia

15 PUBLICATIONS 41 CITATIONS

[SEE PROFILE](#)



Lorenzo Albertazzi

IBEC Institute for Bioengineering of Catalonia

32 PUBLICATIONS 805 CITATIONS

[SEE PROFILE](#)



Mauro Gemmi

Istituto Italiano di Tecnologia

109 PUBLICATIONS 783 CITATIONS

[SEE PROFILE](#)

Water Dispersal and Functionalization of Hydrophobic Iron Oxide Nanoparticles with Lipid-Modified Poly(amidoamine) Dendrimers

Adriano Boni,*† Lorenzo Albertazzi,‡ Claudia Innocenti,§ Mauro Gemmi,† and Angelo Bifone†

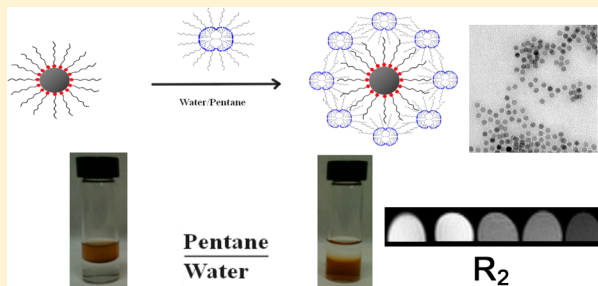
†Istituto Italiano di Tecnologia, Center for Nanotechnology Innovation @NEST, Piazza San Silvestro 12, 56127 Pisa, Italy

‡Institute for Complex Molecular Systems and Laboratory of Macromolecular and Organic Chemistry, Eindhoven University of Technology, P.O. Box 513, 5600 MB, Eindhoven, The Netherlands

§INSTM and Department of Chemistry, University of Florence, via della Lastruccia 3, 50019 Sesto F. no, Firenze, Italy

Supporting Information

ABSTRACT: A novel and facile method for water dispersal of hydrophobic iron oxide nanoparticles based on the amphiphilic PAMAM-C₁₂ dendrimer is described. Stable and highly concentrated water dispersions of multifunctional magnetic nanoparticles were obtained with this single-step approach, and showed interesting relaxometric properties for MRI applications. Importantly, this method does not require substitution of the native hydrophobic capping under nonmild reaction conditions, thus preserving the structural and magnetic properties of the nanoparticles, and extending the possibility of conjugation with thermally labile groups.



INTRODUCTION

Iron oxide superparamagnetic nanoparticles have attracted interest as diagnostic contrast agents (CA) for magnetic resonance imaging.^{1–3} Superparamagnetic nanoparticles induce inhomogeneity in the local field experienced by the surrounding water molecules, thus resulting in shorter T₂ relaxation times of the water protons and in a negative contrast in the MR images.^{4–6} Magnetic nanoparticles are often synthesized by the decomposition of organometallic precursors into hot surfactant solutions, a technique that results in highly crystalline iron oxide cores with a narrow size distribution.^{7–10} However, the resulting powders are dispersible only in nonpolar or moderately polar organic solvents, and the replacement of the hydrophobic coating with a hydrophilic one is necessary to obtaining stable and injectable aqueous solutions. Importantly, the coating should not compromise the nanoparticle magnetic properties. Moreover, the ideal coating should be chemically versatile and easy to conjugate with diverse molecular moieties for the functionalization of the nanoparticle surface. Small molecules such as citric acid¹¹ and dopamine¹² can promote the dissolution of hydrophobic nanoparticles in water, but their stability and versatility for further functionalization are limited. Polymers such as dextran¹³ can be modified more easily to include various functionalities, but the number of exposed groups is not easy to control. Moreover, the replacement of the hydrophobic coating with polymers is a multistep procedure that often requires prefunctionalization of the nanoparticle surface.^{14–16}

Poly(amidoamine) (PAMAM) dendrimers have also been proposed for the coating of magnetic nanoparticles.^{17–20} Dendrimers are highly monodisperse hyperbranched polymers

with a repetitive and perfectly defined structure in which the number and nature of exposed functional groups can be controlled precisely. Moreover, PAMAM dendrimers have been reported²¹ to interact with the surface of the cell membrane and to promote internalization by endocytosis,²² making them a promising tool for therapeutic and diagnostic purposes^{23,24} with a wide range of potential applications such as the intracellular delivery of drugs,^{25,26} genes,^{27–29} and imaging agents.^{30,31}

However, to enable the replacement of the hydrophobic capping (e.g., oleic acid) of the nanoparticles, PAMAM dendrimers are often modified with 1-hexadecaneamine,³² folic acid,¹⁴ or succinic anhydride.²⁰ This ligand-exchange approach suffers from several disadvantages,³³ including poor stability of the aqueous dispersion and the use of nonmild reaction conditions (e.g., 75 °C in DMSO) that limit the possibility to prefunctionalize dendrimers with thermally unstable biomolecules such as certain fluorophores, peptides, and aptamers. Another possible approach is the layer-by-layer self-assembly technique, which requires prefunctionalization of the nanoparticle surface with polymeric layers of polystyrene sulfonate sodium salt (PSS)¹⁷ or poly(glutamic acid) (PGA)/poly(L-lysine) (PLL),¹⁵ involving multistep procedures. However, this method can be applied only to nanoparticles obtained by coprecipitation,³⁴ which is less advantageous than the organometallic decomposition synthesis route.

Here we present a novel and facile method of attaching commercially available lipid-modified PAMAM dendrimers to

Received: March 2, 2013

Revised: April 29, 2013

Published: May 30, 2013



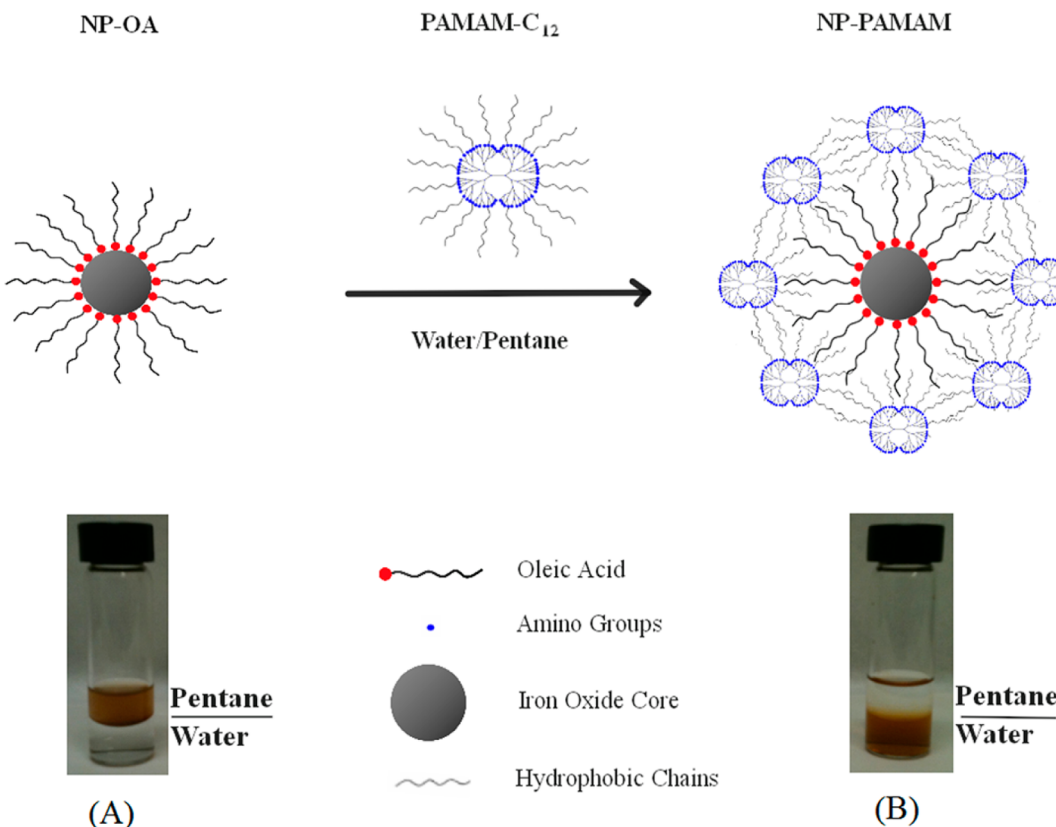


Figure 1. PAMAM- C_{12} coating of the oleic acid-capped iron oxide nanoparticles.

the surface of iron oxide nanoparticles in a single step in a water/pentane mixture at room temperature. We assess the stability of the resulting water dispersion and the structural and magnetic properties of the PAMAM-coated iron oxide nanoparticles. Moreover, we show how these nanoparticle can be used as a very efficient negative contrast agent. Finally, we demonstrate the multifunctionalization of the PAMAM-coated nanoparticles using fluorescent molecules.

RESULTS AND DISCUSSION

Oleic-coated iron oxide nanoparticles (NP-OA) were prepared via a thermal decomposition method, first described by Hyeon et al.,¹⁰ in which the nucleation and growth phases were separate. The coordination of the oleic acid to the nanoparticle surface occurs through chemical bonding of the carboxylic acid group to the metal iron centers,³⁵ as confirmed by FT-IR (data not shown).

Replacement of the oleic acid at the surface of the nanoparticle by the amino groups of unmodified PAMAM dendrimers proved ineffective at room temperature and would require nonmild conditions. An alternative strategy involving the formation of a second layer on the pre-existing oleic acid layer has been recently suggested.^{36–41} This can be obtained through the intercalation of the hydrophobic chains of an amphiphilic molecule in the hydrophobic coating of the nanoparticles. To this end, we chose commercially available PAMAM dendrimers modified with lipid 2-hydroxydodecyl (C_{12}) moieties (Sigma-Aldrich). In particular, we selected a fourth-generation PAMAM dendrimer carrying 48 amino hydrophilic functional groups and 16 hydrophobic C_{12} chains, which was reported to show low toxicity and interesting properties for drug-delivery applications.^{17,42}

The reaction of NP-OA with the PAMAM- C_{12} dendrimers was successfully performed in a water/pentane (1:1) biphasic mixture at room temperature (Figure 1). Pentane was chosen in place of other hydrocarbons, such as hexane, because of its low boiling point, which facilitates its subsequent removal. A 1:30 molar quantity (relative to the oleic acid) of PAMAM- C_{12} dendrimer was dissolved in water and added to a suspension of 7.5 mg of NP-OA (23% Fe via ICP-MS) in pentane. The initial colorless water phase became progressively orange as the nanoparticles were transferred from the pentane to the water phase. After 16 h of vigorous stirring, the organic phase was colorless and the reaction could be stopped. Following pentane removal, the water suspension was dialyzed to eliminate unreacted dendrimer molecules. To the best of our knowledge, this is the first example of a dendrimer-assisted water dispersion of oleic acid-coated nanoparticles performed with a single-step procedure in water/pentane at room temperature.

The final orange solution, obtained in high yield (8 mL, 1.5 mM Fe via ICP-MS) and named NP-PAMAM, was characterized by FT-IR, TEM microscopy, SQUID, and DLS.

Solid-state FT-IR spectroscopy of the NP-PAMAM dry powders corroborates the hypothesis of the hydrophobic interaction of the C_{12} chains of the dendrimer with the oleic acid coating (Figure 2).

The presence of the dendrimer was confirmed by the absorption peaks at 1642 and 1547 cm^{-1} , corresponding to the carbonyl amide and the C–N stretching, respectively, with slight shifts from the bands of the pure PAMAM- C_{12} dendrimer (1637 and 1542 cm^{-1} , respectively). The absorption peak at 1717 cm^{-1} is a clear indication of the permanence of oleic acid on the iron oxide nanoparticle surface, with a shift from the band of free oleic acid (1782 cm^{-1}) and a lower intensity due to

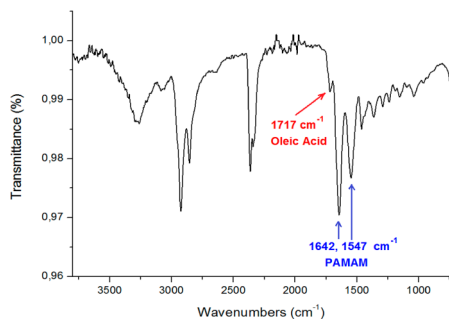


Figure 2. Solid-state FT-IR spectrum of NP-PAMAM displaying typical absorptions of PAMAM- C_{12} at 1642 and 1547 cm^{-1} and of oleic acid at 1717 cm^{-1} .

the coordination to the iron oxide surface. These data demonstrate that PAMAM- C_{12} has not replaced the coordinated oleic acid and suggest that the dendrimer has formed a second layer on the nanoparticle, bound to the first one through hydrophobic interactions.

Notably, nonamphiphilic dendrimers ($G4\text{-NH}_2(64)$) under the same conditions do not bind to NP-OAs, which is a confirmation of the crucial role of the C_{12} chains in the formation of stable interactions with the surface of the NP-OAs.

Interestingly, the lipid-modified dendrimer per se is characterized by relatively poor water solubility,⁴³ and the NP-PAMAM water suspension could be concentrated up to 10 mg/mL Fe without the formation of a precipitate. This suggests that, upon binding to the nanoparticle surface, the coating dendrimers assume a conformation with the hydrophilic portion exposed to the external environment and with most

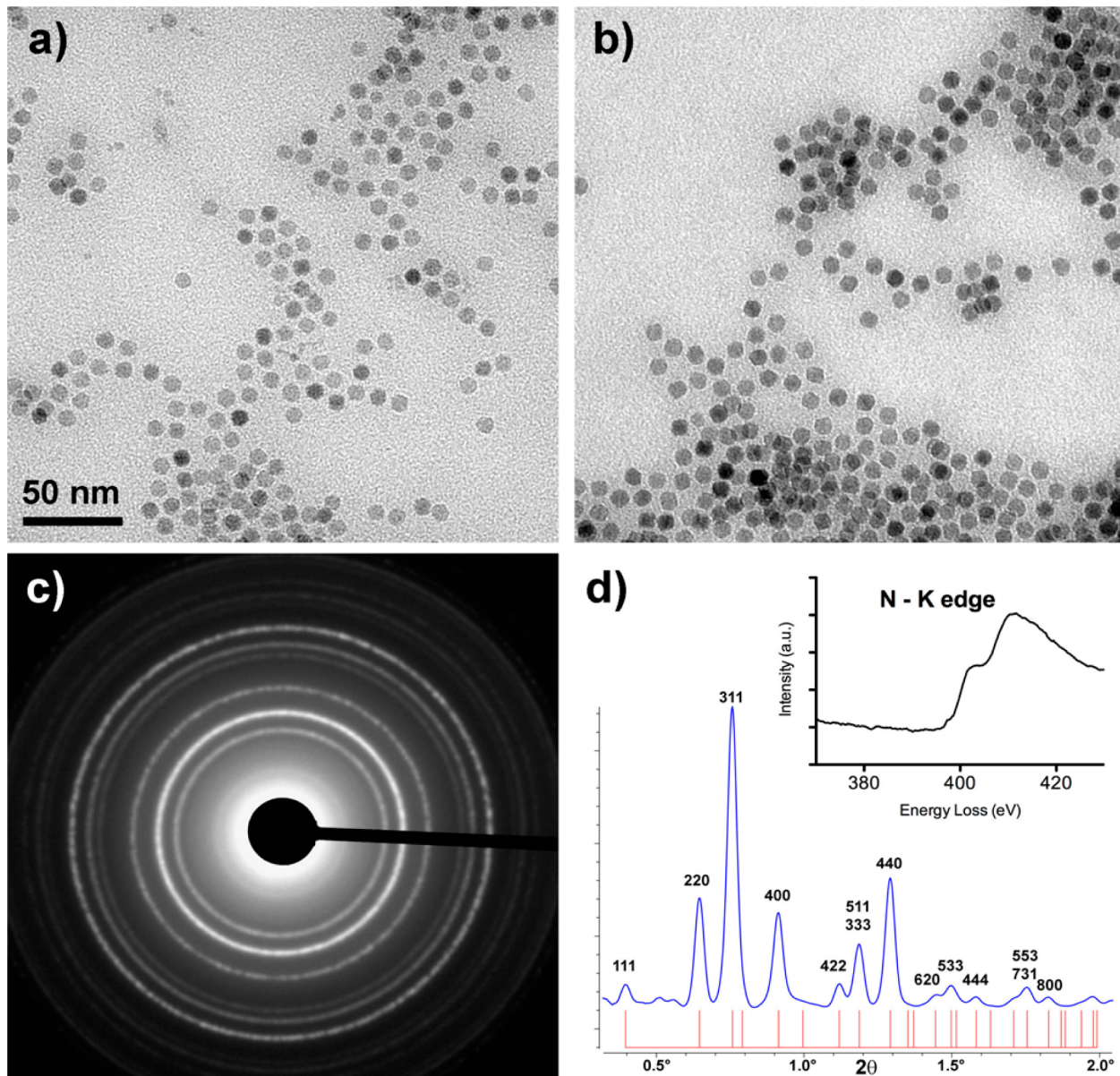


Figure 3. TEM images of NP-OA (a) and NP-PAMAM (b) (both images were taken at the same magnification). Electron diffraction pattern of an assembly of NP-PAMAM (c) and the radially integrated diffraction profile plotted as a function of the 2θ scattering angle (d). Each peak is indexed on the basis of a cubic magnetite structure. The positions of the diffraction peaks calculated for a magnetite structure are indicated by red lines at the bottom. (Inset of d) EELS spectrum collected over an area of 600 nm in diameter rich in NP-PAMAM showing a clear N K-edge.

of the hydrophobic chains pointing toward the oleic acid layer. Also, this configuration does not allow the formation of aggregated nanostructures because the positively charged amino groups provide interparticle repulsion and hydrophobic interactions are limited by the small number of chains pointing toward the external environment.

The TEM micrographs in Figure 3 show the structural characteristics of the iron oxide nanoparticles in the NP-OA (a) and NP-PAMAM (b) samples. Both samples consisted of a dispersion of almost spherical particles. The size distribution over ca. 200 nanoparticles for each sample could be fitted to a Gaussian curve centered on a mean diameter of 8.3 nm, with a standard deviation of 0.5 (Supporting Information). Taking into account the magnetite density (5.15 g/cm^3), we calculated the mass of a single nanoparticle, which was $1.5 \times 10^{-18} \text{ g}$.

ICP-MS analysis of the dry powder of NP-OA and NP-PAMAM allowed us to obtain the iron content and to calculate the remaining amounts of coatings in the samples, which were 67 and 82%, respectively. From the former percentage, we calculated approximately 2 g of OA per 1 g of magnetite, and from the latter, we obtained the sum PAMAM + OA per 1 g of magnetite, which was equal to 4.5 g. Combining these data with the nanoparticle mass, we calculated approximately 6500 molecules of oleic acid and 120 molecules of PAMAM per particle. This is compatible with a system made of large nanoparticles of radius $R = 8.3 \text{ nm}$ surrounded by spherical PAMAM dendrimers of radius 4.5 nm (from Dendritech). The number of spheres of radius r surrounding a sphere of radius R can be estimated by $N = (4\pi(r+R)^2)/r^2$, which in our case is equal to ca. 100. The small discrepancy may be ascribed to the fact that the effective nanoparticle will have a higher effective radius due to its organic coating (thus, R may be higher than 8.3 nm) and the fact that PAMAM is not a rigid sphere but may exhibit a small compression when packed close to other dendrimers (thus, r may be smaller than 4.5 nm).

Finally, an analysis of the electron diffraction pattern of NP-PAMAM (Figure 3c,d) demonstrated that the nanoparticles were crystalline and their diffraction was compatible with a cubic magnetite structure, thus confirming that the PAMAM-C₁₂ coating and water dispersal did not alter the nanoparticles' structure. A Le Bail⁴⁴ fit of the integrated pattern gives a unit cell parameter of $a = 8.409 \pm 0.005 \text{ \AA}$. An EELS spectrum collected on an aggregate of NP-PAMAM shows a clear N K-edge (Figure 3d), not detectable in the case of NP-OA, that can be attributed to the N contained in the amino and amido functionalities of PAMAM-C₁₂, thus providing direct evidence of the presence of the dendrimer coating.

The magnetization of NP-OA and NP-PAMAM as a function of the applied field was measured at 300 K in solid samples (dry powder) using a Quantum Design Ltd. SQUID magnetometer (Figure 4). Both samples displayed superparamagnetic behavior and a high magnetic moment. The saturation values, obtained by fitting the high-field data with empirical law $M = M_s + b/H + c/H^2$ ⁴⁵ and normalizing to the iron content, were 76 emu/g for NP-OA and 73 emu/g for NP-PAMAM, to be compared with bulk magnetite (92 emu/g). The small difference between the two samples was within the experimental error, mainly determined by the accuracy in the measurement of iron concentration, and confirms that the particle structural and magnetic properties were preserved under the mild conditions required by our coating method.

Dynamic light scattering (DLS) analysis was performed to measure the average hydrodynamic diameter of NP-PAMAM

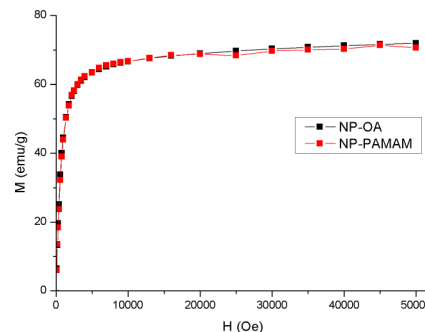


Figure 4. M vs H curves measured at 300 K for powders of NP-OA and NP-PAMAM.

nanostructures and their stability in time. The average size of the magnetite nanoparticles obtained from the DLS mass distribution was 70 nm. The discrepancy with the TEM images may be ascribed to well-documented^{46–49} DLS overestimation due to high scattering from larger particles and from the solvent second coordination sphere. Repeated DLS measurements did not show changes in the mean hydrodynamic diameter over 2 months, thus demonstrating the stability of the colloidal dispersion of NP-PAMAM. These results are very promising in light of a potential application of dendrimer coatings for biomedical applications.

To demonstrate the possibility to use our NP-PAMAM nanoparticles as MRI contrast agents, we performed relaxometric measurements at 300 MHz by means of a Bruker PharmaScan 7 T imager (details in Supporting Information). The results of the MRI measurements are reported in Figure 5. Both longitudinal R_1 and transverse R_2 relaxation rates, defined as the inverse of relaxation times T_1 and T_2 , display a linear increase with concentration, as expected from theory. Intrinsic relaxivities r_1 and r_2 , defined as the relaxation rates at a 1 mM Fe concentration of P904, were inferred from the slope of the regression line, resulting in values of 0.75 ± 0.05 and $112.4 \pm 0.8 \text{ mM}^{-1} \text{ s}^{-1}$, respectively. These results are notable when compared to those reported⁵⁰ for other commercially available iron oxide nanoparticle-based MRI contrast agents in the same field, displaying a high r_2/r_1 ratio (150) that prefigures our NP-PAMAM as a very efficient negative contrast agent.

The ease and versatility of functionalization are important features of NP coatings. To this end, Baker and co-workers proposed an elegant strategy based on the functionalization of the dendrimer prior to the coating process.¹² This approach makes it possible to functionalize the dendrimer in nonaqueous solutions and to characterize the products using techniques such as NMR that are not applicable in the presence of magnetic NPs, thus improving control over the process. However, the subsequent steps in attaching the modified dendrimers to the NPs require high temperatures ($>70^\circ\text{C}$), and this strategy is effective only with thermally stable biomolecules. Moreover, this process requires solvents such as DMSO that are not biocompatible and may remain in traces in the final product, compromising its use in biomedical applications. Here we show that Baker's approach can be easily applied to our C₁₂-modified dendrimer coating and demonstrate a controlled double functionalization of highly crystalline and monodisperse iron oxide nanoparticles at room temperature in a water/pentane mixture. Specifically, we labeled two separate batches of G4-C₁₂ dendrimers with either fluorescein or rhodamine dyes.⁵¹ Subsequently, these dendrimers were

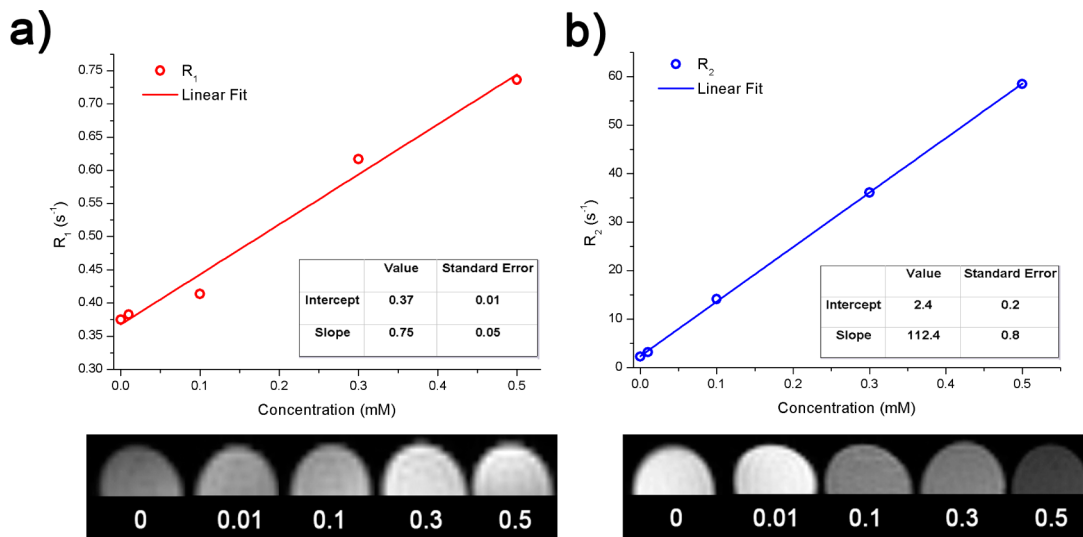


Figure 5. Linear fitting of R_1 (a) and R_2 (b) relaxation rates obtained by the analysis of T_1 -weighted and T_2 -weighted MR images of NP-PAMAM water suspensions at 300 MHz with different concentrations of nanoparticles allowed to estimate the r_1 and r_2 relaxivities.

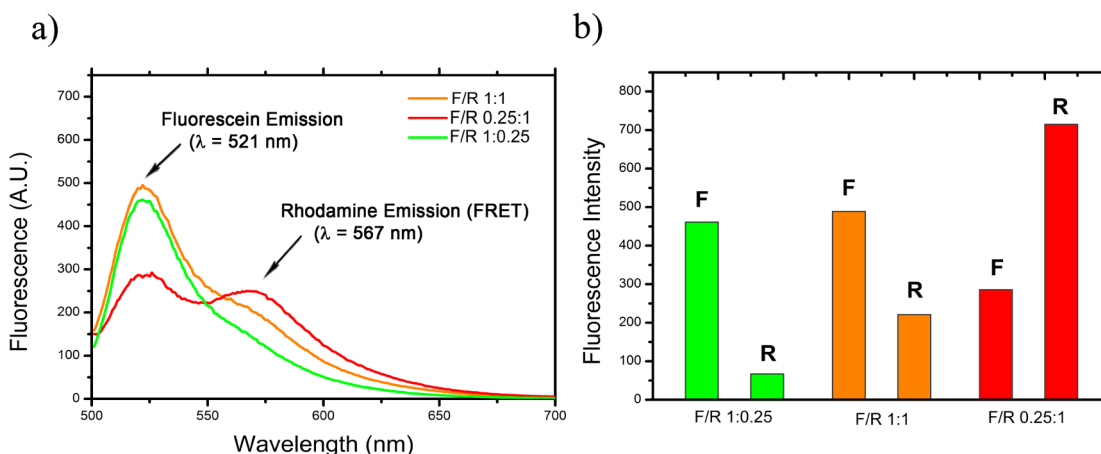


Figure 6. Fluorescence emission spectra (excitation wavelength = 488 nm) of NPs loaded with different fluorescein/rhodamine (F/R) dendrimer molar ratios (a). Histogram reporting fluorescence intensities of fluorescein (F) and rhodamine (R) for different F/R ratios (b).

coloaded onto nanoparticles using our coating method. The loading ratio of the two dendrimers depends on the relative concentrations in the water phase and can be controlled accurately. Figure 6b shows a histogram of the fluorescence emission of nanoparticles with different molar ratios of fluorescein and rhodamine dendrimers (F/R) ranging from 0.25:1 to 1:0.25 after the removal of the unbound dendrimer by dialysis. A clear correlation of the fluorescence intensities with the F/R ratio is apparent. Moreover, a strong FRET band appears at high rhodamine loading (Figure 6a), indicating the proximity of the two dyes and demonstrating the copresence of the two dendrimers on the same NP. These measurements demonstrate that different functionality can be easily introduced onto the NPs and their relative amounts can be tuned by simple stoichiometric control during loading.

CONCLUSIONS

We have reported a novel method of dispersing hydrophobic magnetic nanoparticles in water using a modified C₁₂-PAMAM dendrimer as a coating. This approach enabled us to obtain stable, highly concentrated NP water dispersions that displayed favorable properties as negative contrast agents. We also

demonstrated the possibility of the simultaneous conjugation of different functional groups to the PAMAM-coated NPs using fluorescent molecules as an example.

This method may be extended, in principle, to any nanostructured system with a hydrophobic coating, and presents important advantages over existing strategies. First, our coating and dissolution procedures do not require harsh conditions, thus preserving the magnetic and structural properties of the iron oxide nanoparticles. Moreover, the possibility of performing the coating process directly in water/pentane makes it possible to avoid toxic solvents such as DMSO and DMF, which are difficult to remove, thus reducing the safety risk derived from their presence in traces in the final injectable solution. Finally, the mild temperatures required by this method make it possible to use dendrimers modified with thermally unstable moieties, thus extending the range of functional groups that can be conjugated with NPs for targeting or sensing.

The versatility and facility of application of this method may make it a valuable tool for the development of magnetic nanoparticles as MR contrast agents, as demonstrated here and for other biomedical applications.

■ ASSOCIATED CONTENT

§ Supporting Information

Detailed experimental procedures. TEM and DLS size distribution. Details of relaxometric measurements. This material is available free of charge via the Internet at <http://pubs.acs.org>.

■ AUTHOR INFORMATION

Corresponding Author

*E-mail: adriano.boni@iit.it. Phone: +39 050 509119. Fax: +39 050 509.

Author Contributions

The manuscript was written through the contributions of all authors. All authors have given approval to the final version of the manuscript.

Notes

The authors declare no competing financial interest.

■ ABBREVIATIONS

PAMAM poly(amido)amine; NHS N-hydroxysuccinimide; OA oleic acid; NP nanoparticle; FT-IR Fourier Transform Infra Red; UV-vis Ultraviolet-visible; TEM Transmission Electron Microscopy; SQUID Superconducting Quantum Interference Device; DLS Dynamic Light Scattering; NMR Nuclear Magnetic Resonance; FRET Förster Resonance Energy Transfer

■ REFERENCES

- (1) Tartaj, P.; Morales, M. P.; González-Carreño, T.; Veintemillas-Verdaguer, S.; Serna, C. J. Advances in magnetic nanoparticles for biotechnology applications. *J. Magn. Magn. Mater.* **2005**, *290*–291, 28–34.
- (2) Pankhurst, Q. A.; Connolly, J.; Jones, S. K.; Dobson, J. Applications of magnetic nanoparticles in biomedicine. *J. Phys. D: Appl. Phys.* **2003**, *36*, R167.
- (3) Mornet, S.; Vasseur, S.; Grasset, F.; Veverka, P.; Goglio, G.; Demourgues, A.; Portier, J.; Pollert, E.; Duguet, E. Magnetic nanoparticle design for medical applications. *Prog. Solid State Chem.* **2006**, *34*, 237–247.
- (4) Merbach, A. E.; Tóth, E. *The Chemistry of Contrast Agents in Medical Magnetic Resonance Imaging*; Wiley: Chichester, U.K., 2001.
- (5) Lee, S.-J.; Jeong, J.-R.; Shin, S.-C.; Kim, J.-C.; Chang, Y.-H.; Chang, Y.-M.; Kim, J.-D. Nanoparticles of magnetic ferric oxides encapsulated with poly(D,L-lactide-co-glycolide) and their applications to magnetic resonance imaging contrast agent. *J. Magn. Magn. Mater.* **2004**, *272*–276, 2432–2433.
- (6) Jun, Y.-w.; Huh, Y.-M.; Choi, J.-s.; Lee, J.-H.; Song, H.-T.; KimKim; Yoon, S.; Kim, K.-S.; Shin, J.-S.; Suh, J.-S.; Cheon, J. Nanoscale size effect of magnetic nanocrystals and their utilization for cancer diagnosis via magnetic resonance imaging. *J. Am. Chem. Soc.* **2005**, *127*, 5732–5733.
- (7) Sun, S.; Zeng, H. Size-controlled synthesis of magnetite nanoparticles. *J. Am. Chem. Soc.* **2002**, *124*, 8204–8205.
- (8) Rockenberger, J.; Scher, E. C.; Alivisatos, A. P. A new nonhydrolytic single-precursor approach to surfactant-capped nanocrystals of transition metal oxides. *J. Am. Chem. Soc.* **1999**, *121*, 11595–11596.
- (9) Qu, H.; Ma, H.; Riviere, A.; Zhou, W.; O'Connor, C. J. One-pot synthesis in polyamines for preparation of water-soluble magnetite nanoparticles with amine surface reactivity. *J. Mater. Chem.* **2012**, *22*, 3311–3313.
- (10) Hyeon, T.; Lee, S. S.; Park, J.; Chung, Y.; Na, H. B. Synthesis of highly crystalline and monodisperse maghemite nanocrystallites without a size-selection process. *J. Am. Chem. Soc.* **2001**, *123*, 12798–12801.
- (11) Sahoo, Y.; Goodarzi, A.; Swihart, M. T.; Ohulchanskyy, T. Y.; Kaur, N.; Furlani, E. P.; Prasad, P. N. Aqueous ferrofluid of magnetite nanoparticles: fluorescence labeling and magnetophoretic control. *J. Phys. Chem. B* **2005**, *109*, 3879–3885.
- (12) Shultz, M. D.; Reveles, J. U.; Khanna, S. N.; Carpenter, E. E. Reactive nature of dopamine as a surface functionalization agent in iron oxide nanoparticles. *J. Am. Chem. Soc.* **2007**, *129*, 2482–2487.
- (13) Paul, K. G.; Frigo, T. B.; Groman, J. Y.; Groman, E. V. Synthesis of ultrasmall superparamagnetic iron oxides using reduced polysaccharides. *Bioconjugate Chem.* **2004**, *15*, 394–401.
- (14) Zhang, Y.; Kohler, N.; Zhang, M. Surface modification of superparamagnetic magnetite nanoparticles and their intracellular uptake. *Biomaterials* **2002**, *23*, 1553–1561.
- (15) Lattuada, M.; Hatton, T. A. Functionalization of monodisperse magnetic nanoparticles. *Langmuir* **2006**, *23*, 2158–2168.
- (16) Borase, T.; Ninjbadgar, T.; Kapetanakis, A.; Roche, S.; O'Connor, R.; Kerskens, C.; Heise, A.; Brougham, D. F. Stable aqueous dispersions of glycopeptide-grafted selectively functionalized magnetic nanoparticles. *Angew. Chem., Int. Ed.* **2013**, *52*, 3164–3167.
- (17) Wang, S. H.; Shi, X.; Van Antwerp, M.; Cao, Z.; Swanson, S. D.; Bi, X.; Baker, J. R. Dendrimer-functionalized iron oxide nanoparticles for specific targeting and imaging of cancer cells. *Adv. Funct. Mater.* **2007**, *17*, 3043–3050.
- (18) Shi, X.; Wang, S. H.; Swanson, S. D.; Ge, S.; Cao, Z.; Van Antwerp, M. E.; Landmark, K. J.; Baker, J. R. Dendrimer-functionalized shell-crosslinked iron oxide nanoparticles for in-vivo magnetic resonance imaging of tumors. *Adv. Mater.* **2008**, *20*, 1671–1678.
- (19) Shi, X.; Thomas, T. P.; Myc, L. A.; Kotlyar, A.; Baker, J. R. Synthesis, characterization, and intracellular uptake of carboxyl-terminated poly(amidoamine) dendrimer-stabilized iron oxide nanoparticles. *Phys. Chem. Chem. Phys.* **2007**, *9*, 5712–5720.
- (20) Landmark, K. J.; DiMaggio, S.; Ward, J.; Kelly, C.; Vogt, S.; Hong, S.; Kotlyar, A.; Myc, A.; Thomas, T. P.; Penner-Hahn, J. E.; Baker, J. R.; Holl, M. M. B.; Orr, B. G. Synthesis, characterization, and in vitro testing of superparamagnetic iron oxide nanoparticles targeted using folic acid-conjugated dendrimers. *ACS Nano* **2008**, *2*, 773–783.
- (21) Seib, F. P.; Jones, A. T.; Duncan, R. Comparison of the endocytic properties of linear and branched PEIs, and cationic PAMAM dendrimers in B16f10 melanoma cells. *J. Controlled Release* **2007**, *117*, 291–300.
- (22) Albertazzi, L.; Serresi, M.; Albanese, A.; Beltram, F. Dendrimer internalization and intracellular trafficking in living cells. *Mol. Pharm.* **2010**, *7*, 680–688.
- (23) Tekade, R. K.; Kumar, P. V.; Jain, N. K. Dendrimers in oncology: an expanding horizon. *Chem. Rev.* **2008**, *109*, 49–87.
- (24) Lee, C. C.; MacKay, J. A.; Frechet, J. M.; Szoka, F. C. Designing dendrimers for biological applications. *Nat. Biotechnol.* **2005**, *23*, 1517–26.
- (25) Majoros, I. J.; Myc, A.; Thomas, T.; Mehta, C. B.; Baker, J. R. PAMAM dendrimer-based multifunctional conjugate for cancer therapy: synthesis, characterization, and functionality. *Biomacromolecules* **2006**, *7*, 572–579.
- (26) Lee, C. C.; Gillies, E. R.; Fox, M. E.; Guillaudeau, S. J.; Fréchet, J. M. J.; Dy, E. E.; Szoka, F. C. A single dose of doxorubicin-functionalized bow-tie dendrimer cures mice bearing C-26 colon carcinomas. *Proc. Natl. Acad. Sci. U.S.A.* **2006**, *103*, 16649–16654.
- (27) Zhou, J.; Wu, J.; Hafdi, N.; Behr, J.-P.; Erbacher, P.; Peng, L. PAMAM dendrimers for efficient siRNA delivery and potent gene silencing. *Chem. Commun.* **2006**, *0*, 2362–2364.
- (28) Mintzer, M. A.; Simanek, E. E. Nonviral vectors for gene delivery. *Chem. Rev.* **2008**, *109*, 259–302.
- (29) Caminade, A.-M.; Turrin, C.-O.; Majoral, J.-P.; Dendrimers, D. N. A. Combinations of two special topologies for nanomaterials and biology. *Chem.—Eur. J.* **2008**, *14*, 7422–7432.
- (30) Xu, H.; Regino, C. A. S.; Koyama, Y.; Hama, Y.; Gunn, A. J.; Bernardo, M.; Kobayashi, H.; Choyke, P. L.; Brechbiel, M. W. Preparation and preliminary evaluation of a biotin-targeted, lectin-targeted dendrimer-based probe for dual-modality magnetic resonance and fluorescence imaging. *Bioconjugate Chem.* **2007**, *18*, 1474–1482.

- (31) Kobayashi, H.; Koyama, Y.; Barrett, T.; Hama, Y.; Regino, C. A. S.; Shin, I. S.; Jang, B.-S.; Le, N.; Paik, C. H.; Choyke, P. L.; Urano, Y. Multimodal Nanoprobe for Radionuclide and Five-Color Near-Infrared Optical Lymphatic Imaging. *ACS Nano* **2007**, *1*, 258–264.
- (32) Zhou, Z.; Huang, D.; Bao, J.; Chen, Q.; Liu, G.; Chen, Z.; Chen, X.; Gao, J. A synergistically enhanced T1-T2 dual-modal contrast agent. *Adv. Mater.* **2012**, *24*, 6223–6228.
- (33) Qu, H.; Caruntu, D.; Liu, H.; O'Connor, C. J. Water-dispersible iron oxide magnetic nanoparticles with versatile surface functionalities. *Langmuir* **2011**, *27*, 2271–2278.
- (34) Sugimoto, T.; Matijević, E. Formation of uniform spherical magnetite particles by crystallization from ferrous hydroxide gels. *J. Colloid Interface Sci.* **1980**, *74*, 227–243.
- (35) Willis, A. L.; Turro, N. J.; O'Brien, S. Spectroscopic characterization of the surface of iron oxide nanocrystals. *Chem. Mater.* **2005**, *17*, 5970–5975.
- (36) Wang, Y.; Wong, J. F.; Teng, X.; Lin, X. Z.; Yang, H. Pulling nanoparticles into water: phase transfer of oleic acid stabilized monodisperse nanoparticles into aqueous solutions of α -cyclodextrin. *Nano Lett.* **2003**, *3*, 1555–1559.
- (37) Swami, A.; Kumar, A.; Sastry, M. Formation of water-dispersible gold nanoparticles using a technique based on surface-bound interdigitated bilayers. *Langmuir* **2003**, *19*, 1168–1172.
- (38) Shen, L.; Laibinis, P. E.; Hatton, T. A. Bilayer surfactant stabilized magnetic fluids: synthesis and interactions at interfaces. *Langmuir* **1998**, *15*, 447–453.
- (39) Pellegrino, T.; Manna, L.; Kudera, S.; Liedl, T.; Koktysh, D.; Rogach, A. L.; Keller, S.; Rädler, J.; Natile, G.; Parak, W. J. Hydrophobic nanocrystals coated with an amphiphilic polymer shell: a general route to water soluble nanocrystals. *Nano Lett.* **2004**, *4*, 703–707.
- (40) Lala, N.; Lalbegi, S. P.; Adyanthaya, S. D.; Sastry, M. Phase transfer of aqueous gold colloidal particles capped with inclusion complexes of cyclodextrin and alkanethiol molecules into chloroform. *Langmuir* **2001**, *17*, 3766–3768.
- (41) Gonzales, M.; Krishnan, K. M. Phase transfer of highly monodisperse iron oxide nanocrystals with Pluronic F127 for biomedical applications. *J. Magn. Magn. Mater.* **2007**, *311*, 59–62.
- (42) Bertero, A.; Boni, A.; Gemmi, M.; Gagliardi, M.; Bifone, A.; Bardi, G. Surface functionalisation regulates polyamidoamine dendrimer toxicity on blood-brain barrier cells and the modulation of key inflammatory receptors on microglia. *Nanotoxicology* **2013**, DOI: 10.3109/17435390.2013.765054.
- (43) Hamilton, P.; Jacobs, D.; Rapp, B.; Ravi, N. Surface Hydrophobic modification of fifth-generation hydroxyl-terminated poly(amidoamine) dendrimers and its effect on biocompatibility and rheology. *Materials* **2009**, *2*, 883–902.
- (44) Le Bail, A. Whole powder pattern decomposition methods and applications: a retrospection. *Powder Diffr.* **2005**, *20*, 316–326.
- (45) Morrish, A. H. *The Physical Principles of Magnetism*; Wiley: New York, 1965.
- (46) Regmi, R.; Gumber, V.; Subba Rao, V.; Kohli, I.; Black, C.; Sudakar, C.; Vaishnava, P.; Naik, V.; Naik, R.; Mukhopadhyay, A.; Lawes, G. Discrepancy between different estimates of the hydrodynamic diameter of polymer-coated iron oxide nanoparticles in solution. *J. Nanopart. Res.* **2011**, *13*, 6869–6875.
- (47) Regmi, R.; Black, C.; Sudakar, C.; Keyes, P. H.; Naik, R.; Lawes, G.; Vaishnava, P.; Rablau, C.; Kahn, D.; Lavoie, M.; Garg, V. K.; Oliveira, A. C. Effects of fatty acid surfactants on the magnetic and magnetohydrodynamic properties of ferrofluids. *J. Appl. Phys.* **2009**, *106*, 113902–9.
- (48) Mefford, O. T.; Carroll, M. R. J.; Vadala, M. L.; Goff, J. D.; Mejia-Ariza, R.; Saunders, M.; Woodward, R. C.; St. Pierre, T. G.; Davis, R. M.; Riffle, J. S. Size analysis of PDMS-magnetite nanoparticle complexes: experiment and theory. *Chem. Mater.* **2008**, *20*, 2184–2191.
- (49) Degen, P.; Shukla, A.; Boetcher, U.; Rehage, H. Self-assembled ultra-thin coatings of octadecyltrichlorosilane (OTS) formed at the surface of iron oxide nanoparticles. *Colloid Polym. Sci.* **2008**, *286*, 159–168.
- (50) Noebauer-Huhmann, I. M.; Kraff, O.; Juras, V.; Szomolanyi, P.; Maderwald, S.; Mlynárik, V.; Thyesohn, J. M.; Ladd, S. C.; Ladd, M. E.; Trattnig, S. MR contrast media at 7tesla - preliminary study on relaxivities. *Proc. Int. Soc. Magn. Reson. Med.* **2008**, *16*, 1457.
- (51) Albertazzi, L.; Storti, B.; Marchetti, L.; Beltram, F. Delivery and subcellular targeting of dendrimer-based fluorescent pH sensors in living cells. *J. Am. Chem. Soc.* **2010**, *132*, 18158–18167.